ACS OMEGA

http://pubs.acs.org/journal/acsodf

Article

Synthesis, Structures, and Solution Studies of a New Class of $[Mo_2O_2S_2]$-Based Thiosemicarbazone Coordination Complexes

Arcadie Fuior, Diana Cebotari, Mohamed Haouas, Jérôme Marrot, Guillermo Minguez Espallargas, Vincent Guérineau, David Touboul, Roman V. Rusnac, Aurelian Gulea,* and Sébastien Floquet*

Cite This: *ACS Omega* 2022, 7, 16547−16560

Read Online

ACCESS | Metrics & More | Article Recommendations | Supporting Information

ABSTRACT: This paper deals with the synthesis, structural studies, and behavior in solution of unprecedented coordination complexes built by the association of a panel of 14 representative thiosemicarbazone ligands with the cluster $[Mo_2O_2S_2]^{2+}$. These complexes have been thoroughly characterized both in the solid state and in solution by XRD and by NMR, respectively. In particular, HMBC $^1H\{^{15}N\}$ and ^1H DOSY NMR experiments bring important elements for understanding the complexes' behavior in solution. These studies demonstrate that playing on the nature and the position of various substituents on the ligands strongly influences the coordination modes of the ligands as well as the numbers of isomers in solution, mainly 2 products for the majority of complexes and up to 5 for some of them.

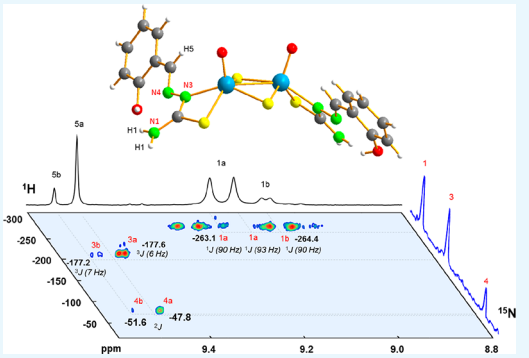

INTRODUCTION

Molybdenum is a very important trace element found in over 50 molybdoenzymes that play numerous roles in living organisms. Nitrogen assimilation by plants, vitamin A formation in mammals, and many other crucial biological redox processes in nature are efficiently performed by these metalloproteins that incorporate Mo(VI) or Mo(V) metallic centers usually embedded within a coordination sphere including sulfur, oxygen, and nitrogen atoms.[1−6] This makes molybdenum very interesting for biochemical and biomedical research. Therefore, developing new Mo-based compounds appears to be a good strategy for developing new drugs, and there are many examples in the literature of the biological activity of Mo-based compounds, including polyoxomolybdates and Mo-coordination complexes.[7−10] In particular, during the past six decades, many authors reported coordination complexes built around the $[Mo^{(V)}{}_2O_2E_2]^{2+}$ (E = O or S) cores with polysulfides and/or polycarboxylate ligands. These clusters are one of the common forms of Mo(+V) cations in solution, and many coordination complexes formed with usual ligands were studied as biomimetic models for redox active centers of molybdoenzymes, notably by Schultz and Ott in the 1960s and 1970s.[11,12] More recently, complexes combining the $[Mo_2O_2S_2]^{2+}$ core and ligands such as polysulfides, cyclopentadiene, DMF, serine, cysteine, or threonine have been suggested to have biological potential by the group of Suman. Their convenient low cytotoxicity on cells was considered useful for possible therapeutic applications like the development of catalytic drugs,[13] especially for cyanide detoxification, for instance.[14−16] Following this work, we recently published a screening study of a series of complexes of $[Mo^{(V)}{}_2O_2E_2]^{2+}$ (E = O or S) with commercial polycarboxylate ligands demonstrating that the biological properties of such complexes strongly depend on the nature of the ligand. For instance, complexes of EDTA were not active for antioxidative properties, while the complexes synthesized with L-cysteine, L-histidine, and iminodiacetate ligands are highly active.[17] These results prompt us to explore new families of complexes with ligands known to be highly bioactive.

For this purpose, our attention turned to thiosemicarbazone molecules. Such ligands are polydentate organic ligands that contain an imine group linked to a thiosemicarbazide moiety (Scheme 1). R1, R2, and R3 groups can be modified as desired, which gives thousands of possibilities. In the past couple of decades, thiosemicarbazone coordination complexes have

Scheme 1. General Representation of Thiosemicarbazone Ligands

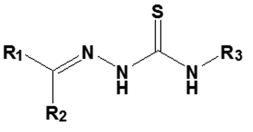

Received: February 3, 2022
Accepted: April 1, 2022
Published: May 3, 2022

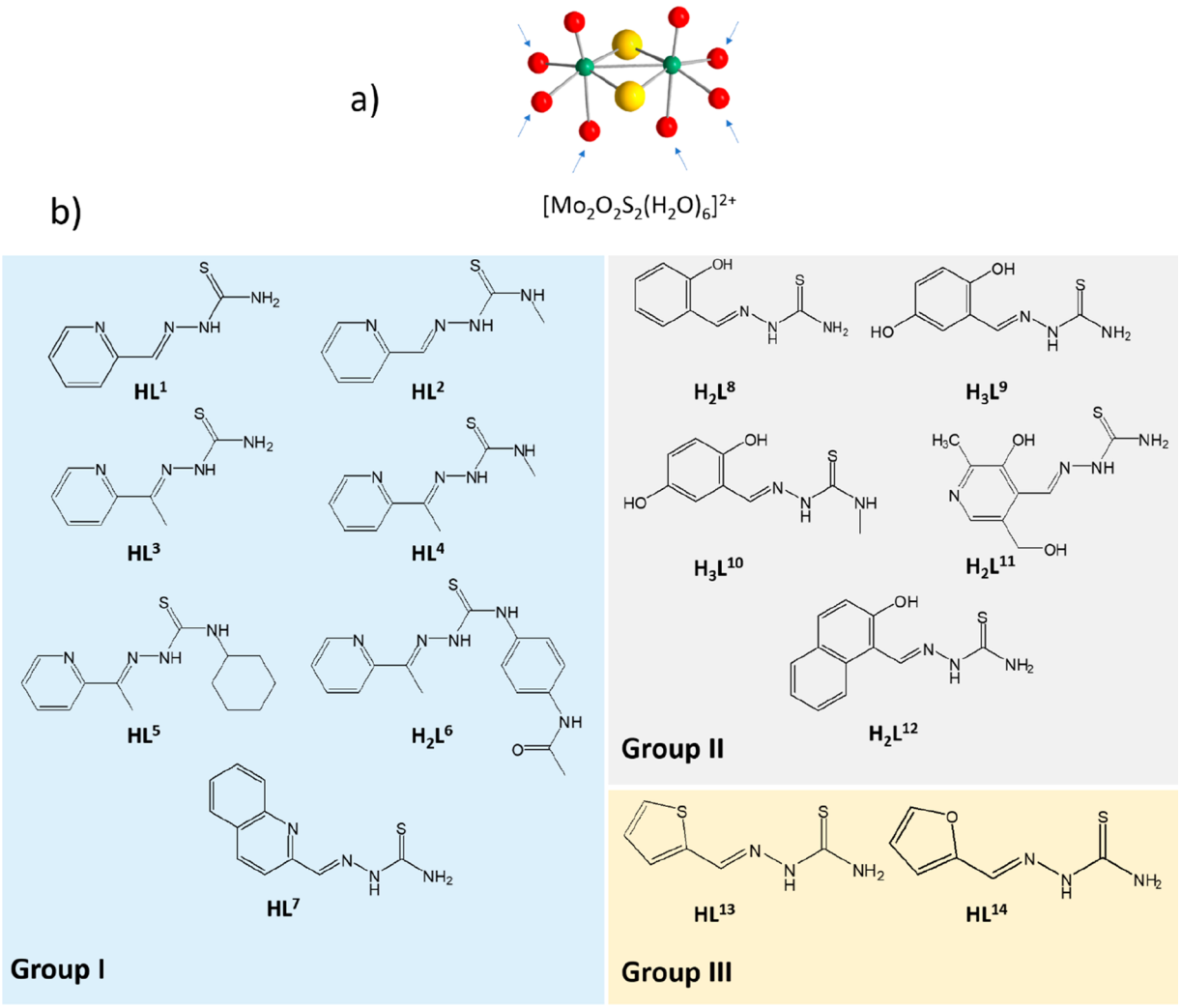

Figure 1. Drawings of (a) the $[Mo_2O_2S_2(H_2O)_6]^{2+}$ cluster highlighting the 6 coordination positions available (arrows) and (b) the 14 thiosemicarbazones ligands used in this study.

received considerable attention in many domains such as molecular magnetism,[18−20] analytical chemistry,[21] biology, or medicine. In particular, thousands of studies gathered in more than 200 reviews were focused in the area of biology and medicine because of the promising biological implications and remarkable pharmacological properties of thiosemicarbazone complexes as antitumor, antiviral, antimalarial, antibacterial, antifungal, or antioxidant agents.[22−38]

Despite the plethora of 3d transition metal thiosemicarbazone complexes reported to date,[39−44] those involving molybdenum are much rarer, although they have been shown to exhibit biological activity.[45−51] In addition, a majority of thiosemicarbazone complexes of Mo contain only one Mo center often found as Mo^{VI}-dioxo moieties, such as $MoO_2(L)(CH_3OH)$-type complexes (where L is a tridentate thiosemicarbazone ligand), which exhibit antioxidant,[46] antitumor,[49] and antibacterial[51] properties. Mo(V) complexes are more scarce.[52−55]

In this context, our work was focused on the preparation of $[Mo^V_2O_2S_2]^{2+}$-based thiosemicarbazone complexes. The dinuclear cluster $[Mo^V_2O_2S_2]^{2+}$ can be used as an electrophilic center with polytopic carboxylate ligands leading to various supramolecular cyclic compounds or with vacant polyoxometalates to give spectacular supramolecular assemblies.[56,57] As seen in Figure 1a, the $[Mo^V_2O_2S_2]^{2+}$ cluster displays 3 available coordination sites on each Mo center, i.e., 2 in the equatorial position and 1 in the axial position, in a position *trans* to the Mo═O bond. This topology does not favor the reaction with thiosemicarbazone ligands, which usually behave as planar tridentate ligands.[20,42,58] In addition, the chemistry of the $[Mo^V_2O_2S_2]^{2+}$ cluster is usually developed in acidic aqueous solution,[56] while 3d thiosemicarbazone complexes are commonly prepared in alcoholic medium in the presence of base.[42,43] Furthermore, to the best of our knowledge, coordination compounds with thiosemicarbazones containing the $[Mo_2O_2S_2]^{2+}$ thiocation have never been described before, even if some binuclear oxo-bridged Mo-based thiosemicarbazone complexes exist.[53,59]

This study thus aims to tackle the challenge of synthesizing a new family of $[Mo_2O_2S_2]^{2+}$-based coordination complexes with a panel of 14 thiosemicarbazone ligands representative of the very wide thiosemicarbazone family of ligands (see Figure 1b). The work will be focused on structural data analysis and the behavior of the complexes in solution thanks to NMR spectroscopy studies, notably ^{1}H DOSY and HMBC ^{1}H{^{15}N} NMR techniques. The latter is rarely used to our knowledge, but we would like to convince the readers that it could be an

https://doi.org/10.1021/acsomega.2c00705
ACS Omega 2022, 7, 16547−16560

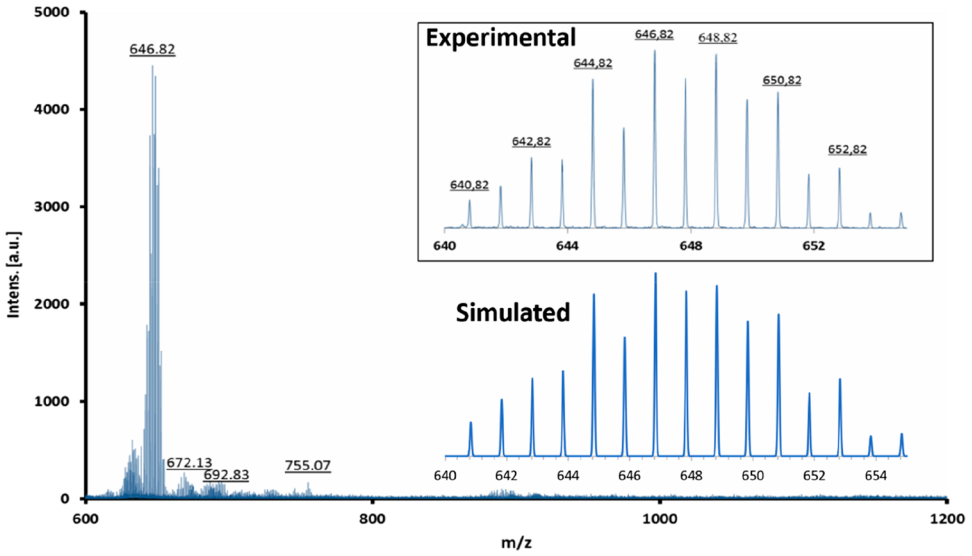

Figure 2. MALDI-TOF spectrum for compound $[\mathbf{Mo_2O_2S_2(L^1)_2}]$. Inset: zoomed-in section of the peak assigned to $[M + H]^+$ species in comparison with the simulated spectrum calculated with Isopro3 software. See Figures S3−S16 in the Supporting Information for the other compounds.

efficient and accessible tool for identifying the nitrogen atoms coordinated to metals.

In the present work, we vary the nature of R1, R2, and R3 groups (see Scheme 1) and divide the ligands into 3 groups for more clarity in the discussion. In particular, R1 will be pyridine or quinoline derivatives (group I, ligands HL^1−HL^7), phenol or naphthol derivatives (group II, ligands H_2L^8−H_2L^{12}), or thiophene or furan derivatives (group III, HL^{13} and HL^{14} ligands). For group I, the R2 group will be −H or −Me to see the effect of functionalization of the ligand on this position, while R2 = H is for ligands of groups II and III. Finally, mainly in group I, the R3 group will change between H, methyl, cyclohexyl, and phenyl-acetamide to evaluate the influence of substitution of this position on the ligand.

RESULTS AND DISCUSSION

Syntheses. The thiosemicarbazone ligands have been well-known since the 1960s. For this study, 14 ligands were selected among hundreds of molecules. These 14 ligands are representative of the large variety of existing ligands in the literature and are prepared by condensation of aromatic and heterocyclic aldehydes and ketones with thiosemicarbazides in methanol or ethanol as described in the Experimental Section (Supporting Information).

The coordination of thiosemicarbazone ligands to the $[Mo_2O_2S_2]^{2+}$ thiocation is not straightforward. Indeed, the cluster $[Mo_2O_2S_2]^{2+}$ is not isolated and is usually found in 1 M HCl aqueous solution,[57] while the thiosemicarbazone ligands are deprotonated in basic medium.[58] Mixing both reactants in acidic medium and increasing the pH lead first to the formation of oxothiomolybdenum cycles which can be partially avoided in large excess of ligand. This approach is not satisfying. Therefore, we developed a novel synthetic route to combine the different reactivities of both components. Specifically, the target complexes were obtained by dropwise addition of a freshly prepared clear yellow-orange aqueous solution of the polyoxothiomolybdate cyclic precursor $(NMe_4)_{0.5}K_{1.5}[I_2Mo_{10}O_{10}S_{10}(OH)_{10}(H_2O)_5]\cdot 20H_2O$ (denoted hereafter Mo_{10})[60] to a hot alcohol solution (methanol or ethanol, see the Experimental Section in the SI) of the ligand (2 equiv per $\{Mo_2O_2S_2\}$ fragment). This precursor appears to be very convenient for this purpose since the 10 hydroxo bridges connecting the 5 $[Mo_2O_2S_2]^{2+}$ units are basic enough to deprotonate the thiosemicarbazone ligands, and at the same time, this process leads to the hydrolysis of the Mo-ring to provide 5 $[Mo_2O_2S_2]^{2+}$ units which can then react with monodeprotonated ligands. The mixture is continuously stirred and heated at 60 °C for 2 h.

In all cases, the compounds are poorly soluble or insoluble in water/alcohol mixtures and are isolated as yellow powders, filtered, washed with ethanol, dried with diethyl ether, and characterized by FT-IR, EDX, and elemental analysis (see the Experimental Section, SI). EDX and elemental analyses (C, H, N, S) carried out on the powders (see Table S2) agree with neutral complexes with the general formula $[Mo_2O_2S_2(H_{x-1}L)_2]$ (x = 1−3) which combine one $[Mo_2O_2S_2]^{2+}$ cluster with two of whichever monodeprotonated ligand is used. For compounds $[\mathbf{Mo_2O_2S_2(L^3)_2}]$, $[\mathbf{Mo_2O_2S_2(L^4)_2}]$, and $[\mathbf{Mo_2O_2S_2(HL^6)_2}]$ some traces of a neutral cyclic cluster $[Mo_{12}O_{12}S_{12}(OH)_{12}(H_2O)_6]$ ("Mo_{12}") are also detected. The latter is almost insoluble and is therefore difficult to separate from the target neutral complexes. It can be formed by reorganization of the Mo_{10} cycle in water, which necessitates the use of a very freshly prepared solution of Mo_{10} for the synthesis of complexes to avoid its formation. MALDI-TOF spectra were measured in the positive mode for all of the compounds (Figure 2 and Figures S3−S16), observing major species corresponding to protonated or sodium-cationized species (see Table S3). The isotopic distribution is in perfect agreement with a dimolybdic cluster, and the results perfectly agree with the formation of neutral $[Mo_2O_2S_2(H_nL^x)_2]$ complexes. Furthermore, it rules out the hypothesis of the formation of more sophisticated species including larger clusters.

Structures. The thiosemicarbazone ligands used (see Figure 1b) possess at least 5 donating functional groups capable of coordination: 1 from the initial aldehyde/ketone part (R1 on Scheme 1), which can be either a pyridine/quinoline group (group I), a phenolic group (group II), or a

https://doi.org/10.1021/acsomega.2c00705
ACS Omega 2022, 7, 16547−16560

thiophene/furan group (group III); and 4 others on the thiosemicarbazide part where the coordination can take place on (i) the imine nitrogen atom —HC=*N*—, (ii) the hydrazinic nitrogen atom =N—*N*H— that can also be azomethinic =N—*N*=CSH because of the thione−thiol tautomer equilibrium, (iii) the thioamide terminal nitrogen atoms —CS(−)—*N*H$_2$ or —CS(−)—*N*HR, and (iv) the sulfur atom usually in the thiol —SH form, which is deprotonated as thiolate for coordination. Usually, 3d transition metal complexes of such ligands involve tridentate planar binding modes with the coordination of metal to thiolate, imine, and the function provided by the aldehyde/ketone part R1. In this study, due to the topology of the cluster $[Mo_2O_2S_2]^{2+}$, three positions are available on each Mo(V) center, but they are not located on the same plane (see Figure 1a). Therefore, unusual coordination modes are expected for such complexes, making it essential to obtain structural details.

Crystals suitable for X-ray diffraction studies were obtained by diffusion of water into DMSO or DMF solutions of compounds $[Mo_2O_2S_2(L^2)_2]$, $[Mo_2O_2S_2(HL^6)_2]$, $[Mo_2O_2S_2(L^7)_2]$, $[Mo_2O_2S_2(HL^8)_2]$, $[Mo_2O_2S_2(HL^{12})_2]$, and $[Mo_2O_2S_2(L^{13})_2]$, i.e., structures involving ligands of all three groups.

Except for the molecular structure obtained with ligand H_2L^6, all of the other molecular structures of complexes exhibit similar features: Each molecular structure (see Figures 3, 5, and 6) involves one $[Mo_2O_2S_2]^{2+}$ fragment coordinated to two ligands in agreement with MALDI-TOF experiments performed on the powders. The formulas determined in powders are maintained except for solvate molecules which become DMF/DMSO and water molecules instead of water and alcohols. The Mo atoms of the $[Mo_2O_2S_2]^{2+}$ cluster are in a distorted square pyramid geometry. The Mo—Mo (range 2.818−2.844 Å), Mo—S (range 2.302−2.338 Å), and Mo=O (range 1.667−1.692 Å) distances perfectly agree with the preservation of the dinuclear unit $[Mo^V_2O_2S_2]^{2+}$.[56,57] Furthermore, the bond valence sum calculations (see Table 1) confirm the oxidation state of Mo (BVS in the 5.06−5.11 range, see Table 1). From their side, the ligands act as bidentate ligands involving the thiolate group and one nitrogen atom of the thiosemicarbazide moiety. The comparison of selected bond lengths between free and coordinated ligands evidences a significant increase of C—S bond length passing from 1.649 to 1.697 Å for the C=S bond in uncoordinated ligands to 1.738−1.769 Å in complexes in agreement with single C—S bonds, while the newly formed π bond between C and hydrazinic N atoms shortens their interatomic distance from 1.335 to 1.369 Å in free ligands to 1.294−1.339 Å in complexes according to the formation of the —N=C(S—)— group. This confirms the formation of monodeprotonated ligands upon reaction with the Mo_{10} precursor and, more precisely, the deprotonation of the hydrazinic NH group and the formation of a thiolate group instead of the thione function of the free ligand. Moreover, the Mo—S(ligand) distances are in good agreement with the distances expected between Mo(V) centers and thiolate groups (see Table 1).[52−55] The second coordination of the ligand to the Mo(V) atoms is ensured by nitrogen atoms, but the coordination modes vary as a function of the nature of the ligand. Surprisingly, the R1 group remains uncoordinated in all cases, while this group is usually involved in coordination complexes of 3d transition metals.[20,42,58]

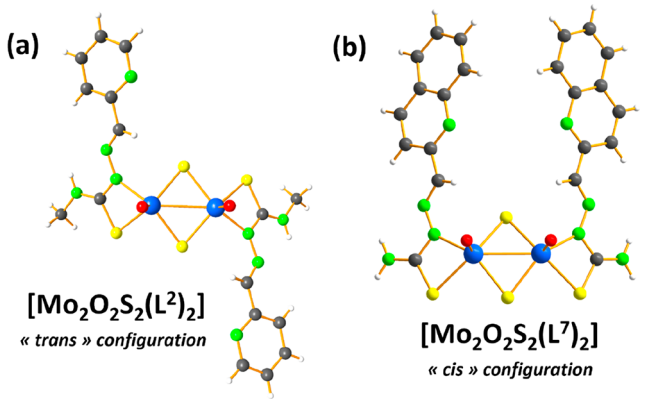

Figure 3. Molecular structures of complexes $[Mo_2O_2S_2(L^2)_2]$ (a) and $[Mo_2O_2S_2(L^7)_2]$ (b). Color code: Mo (blue), C (gray), O (red), N (green), S (yellow), and H (white).

Structures with "Group I" Ligands. Figure 3 shows the molecular structures obtained for complexes of pyridinaldehyde and quinolinaldehyde thiosemicarbazone ligands, namely, $[Mo_2O_2S_2(L^2)_2]$ (Figure 3a) and $[Mo_2O_2S_2(L^7)_2]$ (Figure 3b), respectively. In both cases, the ligands are bidentate and are coordinated in the two equatorial positions of each Mo(V) center by thiolate groups and the azomethinic N atoms, thus forming a 4-atom cycle with Mo(V) atoms. Classically, the thiosemicarbazone ligands coordinate by the thiolate group, by the N-imino atom, and by the R1 function (pyridine, phenol,

Table 1. Selected Bond Lengths around Mo Atoms (Å)

complex	label	C—S	(N)*N*=C(S)	Mo—N	Mo—S$_{ligand}$	Mo—S$_{bridges}$	Mo=O	BVS[a]
$[Mo_2O_2S_2(L^2)_2]$	Mo1	1.748	1.339	2.126	2.452	2.303, 2.337	1.675	5.08
	Mo2	1.742	1.337	2.126	2.453	2.334, 2.303	1.668	5.12
$[(Mo_2O_2S_2(L^6)(DMSO))_2]$	Mo1	1.767	1.292	2.088	2.444	2.306, 2.338	1.690	5.09
	Mo2			2.342, 2.251		2.306, 2.332	1.693, 2.179, Mo—O$_{DMSO}$	5.03
$[Mo_2O_2S_2(L^7)_2]$	Mo1	1.740	1.336	2.132	2.457	2.313, 2.316	1.672	5.10
	Mo2	1.738	1.342	2.123	2.462	2.312, 2.321	1.676	5.08
$[Mo_2O_2S_2(HL^8)_2]$	Mo1	1.740	1.321	2.128	2.453	2.335, 2.310	1.670	5.09
	Mo2	1.747	1.326	2.129	2.460	2.303, 2.329	1.674	5.03
$[Mo_2O_2S_2(HL^{12})_2]$	Mo1	1.729	1.315	2.139	2.474	2.330, 2.314	1.670	5.04
	Mo2	1.732	1.320	2.129	2.451	2.304, 2.324	1.669	5.11
$[Mo_2O_2S_2(L^{13})_2]$	Mo1	1.750	1.319	2.216	2.388	2.337, 2.301	1.667	5.09

[a]Bond valence sum calculation for Mo atoms obtained with Platon software.

https://doi.org/10.1021/acsomega.2c00705
ACS Omega 2022, 7, 16547−16560

...). In our case, the N-imino atoms are not coordinated, and the coordination of this N azomethinic atom is thus surprising and unusual in coordination complexes of thiosemicarbazones; however, the Mo−N distances fall within the usual bond lengths (see Table 1). Interestingly, the two ligands are positioned on opposite sides of the cluster $[Mo_2O_2S_2]^{2+}$, therefore making a *trans* isomer for $[\mathbf{Mo_2O_2S_2(L^2)_2}]$, while they appear in the *cis* configuration for $[\mathbf{Mo_2O_2S_2(L^7)_2}]$ (see Figure 3). These two structures show that such complexes can exist at least in two *cis* and *trans* isomeric forms. The pyridine and the quinoline groups are nonprotonated (from a distance analysis) and noncoordinated to the Mo(V) centers. This result also contrasts with 3d transition metal complexes in which these groups are generally involved in bonding with the metal. This freedom could be of interest for biological properties. From the crystalline packing point of view depicted in the SI (XRD section), no $\pi-\pi$ intermolecular contacts between complexes for both compounds are identified, and only intermolecular contacts between solvates (DMF and/or H_2O) and N atoms of pyridine or quinoline groups or between solvates and the terminal thioamido group can be evidenced. Finally, given the very close nature of pyridine-containing ligands HL^1, HL^3, HL^4, and HL^5, the corresponding complexes are expected to present similar coordination modes in *cis* and *trans* arrangements.

In the case of the ligand H_2L^6, the R3 group on the terminal thioamide function of the thiosemicarbazide moiety also contains an amide function which could coordinate a metal. Such a ligand thus exhibits additional donating atoms and steric hindrance, which could provide different structures. The analyses performed on the powder obtained by the reaction of Mo_{10} with the H_2L^6 ligand gives the formula $[\mathbf{Mo_2O_2S_2(HL^6)_2}]$. By recrystallization from a DMSO/water mixture, single crystals of formula $[\mathbf{(Mo_2O_2S_2(L^6)(DMSO))_2}]$ were obtained. This formula does not correspond to that of the product obtained in powder form. This suggests that the precipitate formed during the synthesis is a kinetic product, while a second deprotonation of the ligand can occur during the recrystallization step to give the $(L^6)^{2-}$ ligand. The only possibility to provide a poorly soluble neutral species between $[Mo_2O_2S_2]^{2+}$ and $(L^6)^{2-}$ is a stoichiometric combination. This corresponds to the tetranuclear complex that we obtained, i.e., $[\mathbf{(Mo_2O_2S_2(L^6)(DMSO))_2}]$, which could be the thermodynamic product. As represented in Figure 4, the molecular structure reveals two twice-deprotonated ligands acting as bridging bis(bidentate) ligands that are coordinated to two $[Mo_2O_2S_2]^{2+}$ clusters. On one side, the ligand is coordinated to the labeled Mo1 atom on two equatorial coordination sites by the thiolate group of the ligand and surprisingly by the nitrogen atom of the thioamide N10 atom (see Figure 4), which seems to also be deprotonated. Such deprotonation is unusual, but it could be favored by a mesomeric stabilization by the aromatic R3 group functionalized by a withdrawing amide function. Such a phenomenon is not observed and not possible for the 13 other ligands. On the other side of the ligand, the imine (N11) and the pyridine (N18) N atoms are both coordinated in a classical way to the Mo2 atom belonging to a second $[Mo_2O_2S_2]^{2+}$ cluster. The imine N13 atom is found in the apical position, while the N atom of the pyridine group N21 is linked to the metal through an equatorial coordination site.

The Mo−N13 distance of 2.34 Å appears to be significantly longer than the Mo−N21 distance (2.25 Å), in agreement with

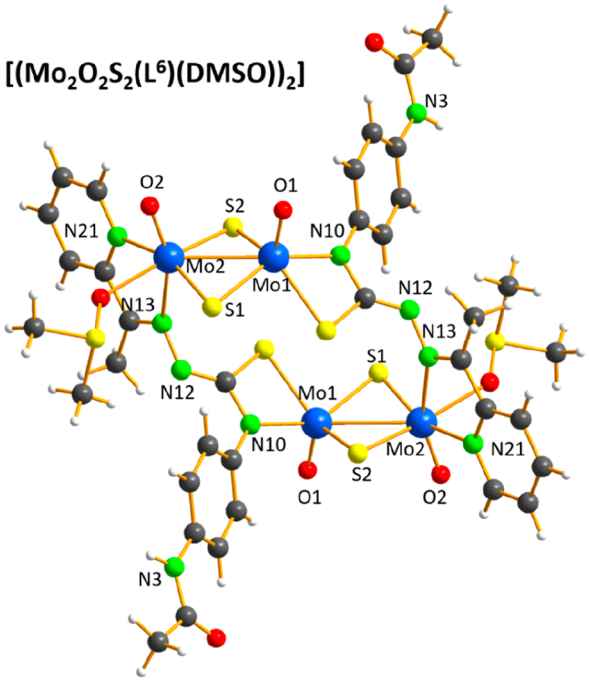

Figure 4. Molecular structure of compound $[(\mathbf{Mo_2O_2S_2})_2(\mathbf{L^6})_2(\mathbf{DMSO})_2]$. Color code: Mo (blue), C (gray), O (red), N (green), and S (yellow).

a *trans* effect on Mo. The coordination sphere of Mo2 is filled by a DMSO molecule on an equatorial position to obtain a distorted octahedral arrangement while Mo1 adopts a distorted square pyramid geometry. Finally, the analysis of the crystalline packing (see the SI, XRD section) reveals partial overlapping between pyridine rings from neighboring complexes and thus $\pi-\pi$ intermolecular contacts between complexes in the solid state (distance in the range 3.3−3.5 Å). This result demonstrates the possibility to obtain original arrangements when bulky appropriate aromatic groups are used in this terminal position of the ligands.

Structures with "Group II" Ligands. In the case of phenolic derivatives, the molecular structures of complexes formed with salicylaldehyde (H_2L^8) and 2-hydroxy-naphtaldehyde thiosemicarbazones (H_2L^{12}) have been solved by XRD. According to MALDI-TOF experiments, complexes with a 1:2 stoichiometry were obtained as depicted in Figure 5. The two Mo atoms of the cluster are pentacoordinated, and the coordination modes are similar to those obtained with the thiosemicarbazone ligands of Group I: Mo atoms in a distorted square planar geometry and thiosemicarbazone ligands coordinated to Mo(V) atoms through thiolate and azomethinic N atoms. In these cases, the two ligands within complexes $[\mathbf{Mo_2O_2S_2(HL^8)_2}]$ and $[\mathbf{Mo_2O_2S_2(HL^{12})_2}]$ display a *trans* arrangement.

In these two molecular structures, unexpectedly for this class of ligands, the ligands do not act as classical tridentate ONS donors. Indeed, in contrast with the number of complexes in the literature, the −OH function of the R1 group remains protonated and noncoordinated to the metal, while it is usually deprotonated and coordinated in 3d transition metal complexes.[20,58,61]

Furthermore, the configuration of the ligand in both complexes could be stabilized by intramolecular contacts between the N imino group with the −OH group from R1

https://doi.org/10.1021/acsomega.2c00705
ACS Omega 2022, 7, 16547−16560

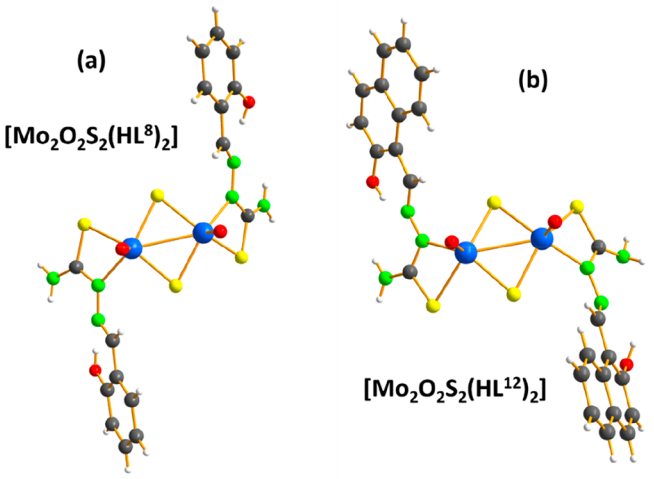

Figure 5. Molecular structures of complexes $[Mo_2O_2S_2(HL^8)_2]$ (a) and $[Mo_2O_2S_2(HL^{12})_2]$ (b). Color code: Mo (blue), C (gray), O (red), N (green), and S (yellow).

(d_{N-O} 2.65 Å in both complexes) and terminal $-NH_2$ group ($d_{N_{imino}-N_{thioamido}}$ = 2.72 and 2.75 Å). Finally, in both cases, H-bonds between −OH and $-NH_2$ functions of the ligands and solvates can be identified in both structures, but there is no evidence of a direct H-bond network or $\pi-\pi$ stacking between complexes.

Structures with "Group III" Ligands. Finally, for the last category of ligands represented by HL^{13}, the molecular complex of a 1:2 stoichiometry gives a *trans*-type isomer with 2 monodeprotonated $(L^{13})^-$ ligands in which the thiophene group is found to be free, in agreement with the structures obtained with HL^1, HL^2, H_2L^8, and H_2L^{12} ligands, and the coordination spheres of the two Mo(V) centers are ensured by the thiolate groups and the imine group of the ligand (Figure 6), while the imine was found uncoordinated in

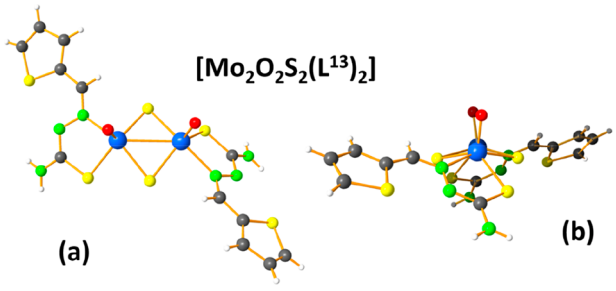

Figure 6. Molecular structure of complex $[Mo_2O_2S_2(L^{13})_2]$: top view (a) and side view (b). Color code: Mo (blue), C (black), O (red), N (green), and S (yellow).

almost all of the other complexes. Such a coordination mode is more usual for this type of ligand with transition metals. Nevertheless, as seen in Figure 6, it provokes a stronger distortion of the coordination sphere of the Mo atoms and also a distortion within the dinuclear cluster evidenced by the two Mo═O bonds which appear to be clearly not parallel. This distortion is very limited in the other structures when azomethinic N atoms are coordinated. This could explain the preferential coordination to the latter rather than the imino N atom.

From the crystalline packing point of view, intermolecular contacts between complexes are ensured through H-bonds involving $-NH_2$ functions of the ligands with S atoms of the R1 groups (d_{S-N} = 3.25 Å) which allows one complex to connect to four neighboring complexes. In contrast with the previous structures, the solvates that usually interact with these groups are highly disordered in this structure and were not positioned confidently.

In summary, as a general feature, the structures combining the cluster $[Mo_2O_2S_2]^{2+}$ with thiosemicarbazone ligands evidence a bidentate behavior of these ligands, a preferential coordination of the ligands at the equatorial positions of the Mo(V) centers, and unusual and sometimes even unprecedented coordination modes for such a class of ligands. We also observe that the aldehyde/ketone part of the ligand, i.e., R1 groups, is noncoordinating regardless of the nature of this group and the possible formation of different isomers, mainly *cis* and *trans* for a 1:2 stoichiometry. In contrast with the other ligands, the structural studies also evidence that a more sophisticated ligand, such as H_2L^6, can induce the formation of a dimeric arrangement of 2:2 stoichiometry with a bridging bis(bidentate) character for the ligand. In this case, the use of an R3 group capable of stabilizing the deprotonation of the thioamido group of the ligands is undoubtedly very important. Finally, the replacement of H by a methyl group as R2 or the use of a thiophene derivative as R1 seems to favor the coordination of the imino N atom to Mo atoms, which adopts either a highly distorted square pyramidal or a distorted octahedral geometry. To confirm these assessments, and to study the formation of different isomers in solution, an NMR study was thus performed in DMSO.

Solution Studies by NMR. Considering (i) the equatorial and axial positions of the two Mo(V) centers, (ii) the presence of two ligands for each complex with 4 or 5 donating atoms on each ligand, and (iii) the evidence by X-ray diffraction studies of the formation of different types of assemblies and isomers, the investigation of properties in solution of $[Mo_2O_2S_2]$-based thiosemicarbazone complexes appears to be necessary to evidence the formation of favored isomers among numerous possible isomers (at least 12 possible isomers just by considering the coordination involving thiolate groups and N azomethinic atoms; see Figure S112 and the corresponding discussion in the SI for more details). The investigations were performed in DMSO by using various NMR techniques including 1D ^1H NMR, 2D ^1H NMR experiments such as ROESY and DOSY, and 2D $^{15}N\{^1H\}$ HMBC correlation NMR. Only a few selected spectra corresponding to the complex $[Mo_2O_2S_2(HL^8)_2]$ as representative example are presented in the main text, while all other NMR spectra are given in the Supporting Information (see the NMR section). The main results are gathered in Table S5, while Tables 2 and 3 summarize data acquired for DOSY and $^{15}N\{^1H\}$ HMBC 2D experiments for ligands and complexes.

As can be seen in Figure 7, a comparison of the ^1H NMR spectra of the free ligand H_2L^8 and the powder analyzed as $[Mo_2O_2S_2(HL^8)_2]$ shows that the chemical shifts of all protons of the ligand have undergone significant changes. Interestingly, the ^1H spectrum of $[Mo_2O_2S_2(HL^8)_2]$ exhibits two sets of signals highlighted by spectral decomposition using the Dmfit NMR tool.[62] The two subspectra display the same features and the same multiplicities in agreement with two identical ligands within the complexes thanks to an inversion center for the *trans* isomer or a symmetry plane passing by the center of the

https://doi.org/10.1021/acsomega.2c00705
ACS Omega 2022, 7, 16547−16560

Table 2. Diffusion Coefficient Values in $\mu m^2/s$ for Ligands and Complexes Measured for a Total Concentration of Ligand of 5 mM in DMSO-d_6

uncoordinated ligands		complexes		
ligand	D ($\mu m^2/s$)	formula[a]	D ($\mu m^2/s$)	calculated r_h hydrodynamic radius of complex[b] (Å)
HL^1	266 ± 8	$[Mo_2O_2S_2(L^1)_2]$	160 ± 9	6.9
HL^2	300 ± 10	$[Mo_2O_2S_2(L^2)_2]$	190 ± 7	5.8
HL^3	290 ± 10	$[Mo_2O_2S_2(L^3)_2]$	190 ± 30	5.8
HL^4	300 ± 20	$[Mo_2O_2S_2(L^4)_2]$	170 ± 20	6.5
HL^5	270 ± 4	$[Mo_2O_2S_2(L^5)_2]$	170 ± 20	6.5
H_2L^6	300 ± 20	$[(Mo_2O_2S_2)(HL^6)_2]$	130 ± 20	8.5
HL^7	243 ± 7	$[Mo_2O_2S_2(L^7)_2]$	157 ± 10	7.0
H_2L^8	230 ± 20	$[Mo_2O_2S_2(HL^8)_2]$	158 ± 5	7.0
H_3L^9	221 ± 3	$[Mo_2O_2S_2(H_2L^9)_2]$	153 ± 6	7.2
H_3L^{10}	229 ± 7	$[Mo_2O_2S_2(H_2L^{10})_2]$	170 ± 10	6.5
H_3L^{11}	250 ± 8	$[Mo_2O_2S_2(H_2L^{11})_2]$	170 ± 20	6.5
H_2L^{12}	230 ± 10	$[Mo_2O_2S_2(HL^{12})_2]$	170 ± 20	6.5
HL^{13}	279 ± 6	$[Mo_2O_2S_2(L^{13})_2]$	175 ± 7	6.3
HL^{14}	291 ± 5	$[Mo_2O_2S_2(L^{14})_2]$	190 ± 10	5.8
		$[Mo_2O_2S_2(HNTA)_2]^{2-}$	173 ± 6	6.4

[a]Formulas are those of powders (without solvates) solubilized in DMSO. [b]Hydrodynamic radii are calculated by using the Stokes−Einstein equation $D = k_BT/6\pi\eta r_h$: k_B Boltzmann's constant, T temperature (K), and η solvent viscosity.

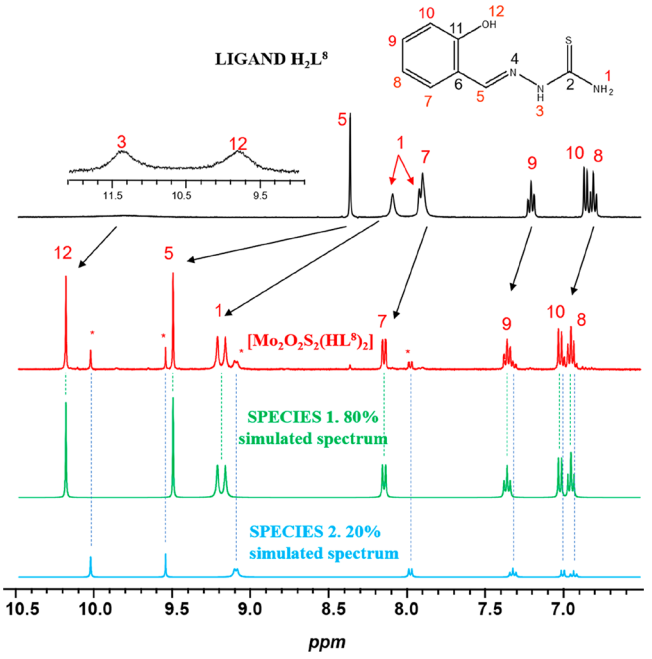

Figure 7. 400 MHz ^1H NMR (DMSO-d_6) spectrum of ligand H_2L^8 (black), complex $[Mo_2O_2S_2(HL^8)_2]$ (red), and the two simulated subspectra contained in $[Mo_2O_2S_2(HL^8)_2]$. Attributions of the ^1H NMR signals of the free ligands were made thanks to the literature data[63] and ROESY experiments when needed, while those of protons in complexes are confirmed by ROESY and by heteronuclear $^1H\{^{15}N\}$ HMBC NMR techniques (see the NMR section in the SI).

Mo−Mo bond for the *cis* isomer. The signals are assigned using literature and NOESY experiments (see the SI). In particular, the cross peaks corresponding to H12−H10 and H5−H7 correlations confirm the assignment of the imine proton as H5 and the presence of the noncoordinated phenol group H12, in agreement with the structure (the labels are given in Figure 7).

The signals of the proton or the methyl group on the imine function of the ligands are sufficiently resolved to serve as a good probe to distinguish a mixture of complexes with their proportions in all of our 14 compounds. In the present case, two species of relative proportions of 20/80 are identified and must correspond to the two position isomers with *cis* and *trans* configurations for the two ligands as the XRD studies revealed. For both species, the aromatic protons (H7−H10) are the least affected (up to 0.3 ppm shifts), while the peaks from the thiosemicarbazide moiety are dramatically shifted downfield. The most sensitive are the imine and thioamide protons (H5 and H1/H1′, respectively), having moved on the spectrum by 1.1−1.3 ppm. It is important to mention that the H3 signal disappeared after complexation in accordance with the deprotonation of the hydrazinic N atoms of the ligand. Unfortunately, it was not possible to assign the *cis* and *trans* isomers to their spectra, even by using different 2D NMR methods (DOSY, NOESY, ROESY, ...).

Similarly, only two species were evidenced for the eight compounds $[Mo_2O_2S_2(L^1)_2]$, $[Mo_2O_2S_2(L^2)_2]$, $[Mo_2O_2S_2(L^7)_2]$, $[Mo_2O_2S_2(HL^8)_2]$, $[Mo_2O_2S_2(H_2L^9)_2]$, $[Mo_2O_2S_2(H_2L^{10})_2]$, $[Mo_2O_2S_2(HL^{11})_2]$, and $[Mo_2O_2S_2(HL^{12})_2]$, which clearly demonstrates that the two *cis* and *trans* isomers are undoubtedly favored in this family of complexes. In contrast, for complexes with 2-acetylpyridine, i.e., when the R2 group of the ligand is a methyl group (ligands HL^3, HL^4, and HL^5), more isomers are observed in solution.

As seen in Figures S42, S48, and S54, the number of isomers increases to 4, 5, and 4 for $[Mo_2O_2S_2(L^3)_2]$, $[Mo_2O_2S_2(L^4)_2]$, and $[Mo_2O_2S_2(L^5)_2]$, respectively. As seen in Figure S42, 4 isomers of $[Mo_2O_2S_2(L^3)_2]$ are observed with two main isomers with relative intensities of 46% and 36%, respectively, and two minor species at 12% and 8%, respectively. The NMR methods did not permit an identification of the type of isomers. For $[Mo_2O_2S_2(L^4)_2]$, the two main isomers represent 55% of the mixture while the three others represent 45% (see Figure S51). Finally, for $[Mo_2O_2S_2(L^5)_2]$ (see Figure S54), the two main isomers correspond to 55% and 25% of the mixture, while the two minor species are found with 13% and 7% proportions.

In the case of ligand H_2L^6, the broadness of some signals precludes a confident determination of the number of isomers (Figure S62). Finally, for complexes of ligands of Group III,

https://doi.org/10.1021/acsomega.2c00705
ACS Omega 2022, 7, 16547−16560

i.e., furaldehyde (HL^{14}) or thiophenaldehyde (HL^{13}), thiosemicarbazone ligands, up to 8 different species are observed for $[Mo_2O_2S_2(L^{13})_2]$ (Figure S99) and 5 isomers for $[Mo_2O_2S_2(L^{14})_2]$ (Figure S107). Note that, for the latter, as shown in the Supporting Information, from two isomers identified in a fresh mixture (Figure S105), the solution slowly evolves to give up to 5 isomers (Figure S107), which suggests a dynamic equilibrium between these species.

Although it was not possible to identify the nature of each isomer, the main results of this solution study are that the preferential isomers are formed in solution. In addition, the number of species clearly depends on the nature of R1 and R2 groups of the thiosemicarbazone ligands. To limit the formation of isomers, R1 must be pyridine, quinoline, phenol, or naphthol derivatives, while R2 must be H (and not Me). Indeed, when R1 = thiophenaldehyde or furanaldehyde, or R2 = Me, in all cases, the number of isomers increases. It should increase the basicity of the N imino atoms and reinforce the competition with N azomethinic atoms for coordination with Mo. This hypothesis agrees well with the results obtained by X-ray diffraction of $[(Mo_2O_2S_2(L^6)(DMSO))_2]$ and $[Mo_2O_2S_2(L^{13})_2]$ (see Figures 4 and 6, respectively), which suggests that the imino N atom can be coordinated when R2 = Me and R1 = thiophene derivative.

^{1}H DOSY NMR proved to be an efficient tool for investigating size and supramolecular assemblies in solution.[64,65] In our case, such an experiment can be useful to demonstrate that the two subspectra seen in Figure 7 correspond to a mixture of two isomers. Diffusion NMR experiments were thus performed on DMSO solutions of free ligands and their corresponding complexes. The diffusion coefficients are gathered in Table 2, while Figure 8 shows the spectra obtained for ligand H_2L^8 and complex $[Mo_2O_2S_2(HL^8)_2]$. Note that the dinuclear complex $[Mo_2O_2S_2(HNTA)_2]^{2-}$, which exhibits a size similar to that of two arms of the nitrilotriacetate (NTA^{3-}) remaining uncoordinated and either *cis* or *trans* positions of the two ligands (Figure 8a) in equilibrium in solution, is chosen as a reference for the diffusion coefficient of dinuclear species.

As shown in Table 2, the diffusion coefficients of the free ligands fall in the range 230−300 $\mu m^2/s$ depending on the size of the ligands. The formation of complexes naturally leads to larger molecular systems. Therefore, the values of diffusion coefficients are found to be lower than those of the free ligands in the range 153−190 $\mu m^2/s$. These values agree with the value expected for dinuclear species and are fully compatible with the reference compound $[Mo_2O_2S_2(HNTA)_2]^{2-}$ showing a value of 173 $\mu m^2/s$. More interestingly, the two subspectra identified by ^{1}H NMR (see Figure 7) exhibit similar diffusion coefficients as those seen in Figure 8b. Such a result is possible for species possessing similar hydrodynamic radii. Therefore, considering the results of the XRD studies, the assignments of the two subspectra agree well with the formation in solution of both *cis* and *trans* isomers of the $[Mo_2O_2S_2(HL^8)_2]$ complex in slow dynamic exchange in DMSO (variable temperature NMR did not modify the proportions of the species). A similar conclusion is made for the seven other compounds $[Mo_2O_2S_2(L^1)_2]$, $[Mo_2O_2S_2(L^2)_2]$, $[Mo_2O_2S_2(L^7)_2]$, $[Mo_2O_2S_2(H_2L^9)_2]$, $[Mo_2O_2S_2(H_2L^{10})_2]$, $[Mo_2O_2S_2(HL^{11})_2]$, and $[Mo_2O_2S_2(HL^{12})_2]$.

For complexes exhibiting more complicated systems with a mixture of up to 8 components (see the SI), the DOSY experiments also suggest a mixture of isomers with comparable

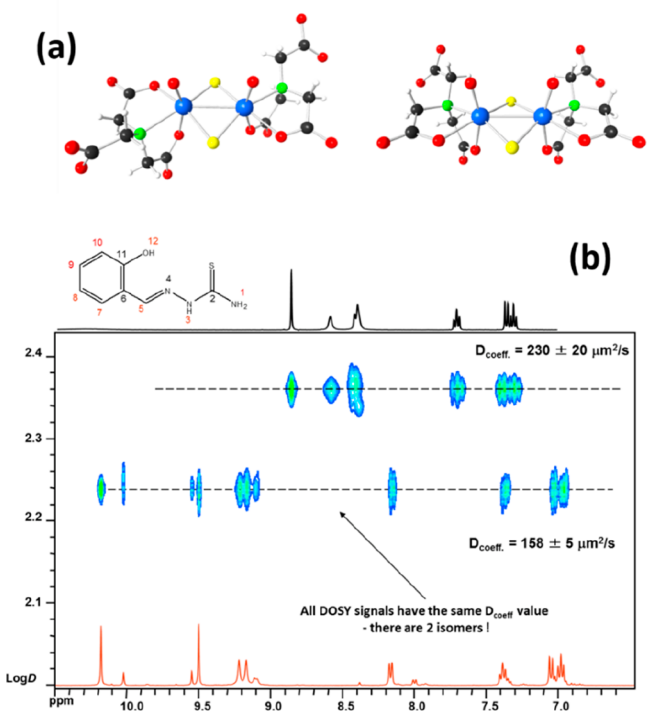

Figure 8. (a) Molecular structures of *cis* and *trans* isomers of $[Mo_2O_2S_2(HNTA)_2]^{2-}$ chosen as a reference. (b) Superimposed 400 MHz ^{1}H DOSY NMR (DMSO-d_6) spectra of ligand H_2L^8 and complex $Mo_2O_2S_2(HL^8)_2$. The ^{1}H NMR spectra of the ligand and complex are given for clarity in black and red, respectively.

diffusion coefficients, which could involve different coordination modes of the ligands, notably the nature of the coordinated N atoms, as well as coordination in both the axial and equatorial positions of Mo centers as depicted in Figure S112. Finally, in the case of compound $[Mo_2O_2S_2(HL^6)_2]$, the diffusion coefficient displays a much lower value of D = 130 $\mu m^2/s$ in agreement with larger species with an average hydrodynamic radius of 8.5 Å, which is an intermediate value between the size of the tetranuclear complex characterized by X-ray diffraction (11 Å) and the common dinuclear complexes (6−7 Å). This suggests for this compound an equilibrium in solution between the two complexes $[Mo_2O_2S_2(HL^6)_2]$ and $[(Mo_2O_2S_2(L^6)(DMSO))_2]$ and also probably some intermediate species and, consequently, averaged D values.

Although ^{1}H NMR techniques have yielded important information on ligand coordination, complex size, and the presence of multiple isomers, such techniques cannot confidently elucidate ligand coordination modes, especially the nature of N atoms bound to the Mo centers. Due to its quadrupolar moment, which leads to broad lines, the ^{14}N nucleus is rarely used in NMR despite a natural abundance of 99.63%. In addition, the ^{15}N isotope exhibits a spin of 1/2, but the sensitivity of ^{15}N is much lower than ^{13}C; the direct 1D NMR measurement is very difficult. HMBC ^{1}H{^{15}N} experiments were developed in the 1990s, and this method has proved beneficial in determining structures of alkaloids and nitrogen atoms involved in coordination processes and protonation.[66,67] It allows the acquisition of a ^{15}N spectrum through the ^{1}H nuclei linked to nitrogen atoms, and it necessitates about 16 h experiments in 10 mM solution to obtain satisfactory data for our study. HMBC ^{1}H{^{15}N}

https://doi.org/10.1021/acsomega.2c00705
ACS Omega 2022, 7, 16547−16560

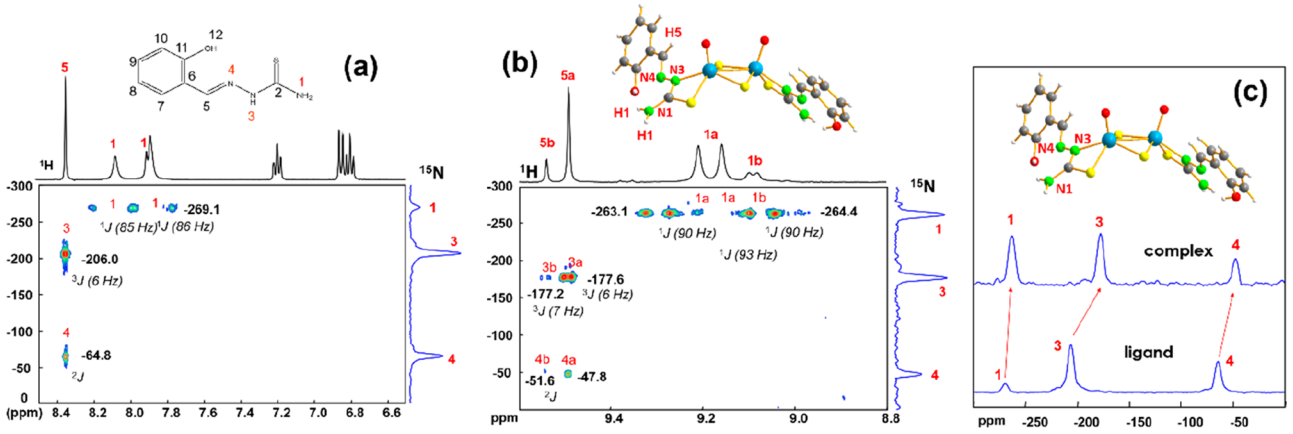

Figure 9. 400 MHz $^{1}H\{^{15}N\}$ HMBC NMR (DMSO-d_6) spectra of ligand H_2L^8 (a) and complex $[Mo_2O_2S_2(HL^8)_2]$ (b) (a and b correspond to the two isomers identified by ^{1}H NMR). (c) Highlight of the chemical shift variation of ^{15}N spectra induced by coordination of the ligand.

experiments not only measure ^{15}N spectra but also provide the correct assignment of both ^{15}N and some ^{1}H peaks. Figure 9 displays the HMBC $^{1}H\{^{15}N\}$ spectra recorded for ligand H_2L^8 and complex $[Mo_2O_2S_2(HL^8)_2]$ in DMSO, while those obtained for the other complexes are given in the Supporting Information. Table 3 lists the ^{15}N NMR chemical shifts obtained for ligands and the main isomer of complexes.

As shown in Figure 9a and the corresponding figures in the SI, the $^{1}H - {}^{15}N$ correlations and the strength of the coupling constant in the ligand allow the unambiguous identification of the signals assigned to the nitrogen atoms within the ligands. In the case of the ligand H_2L^8 (Figure 9a), the signal of the imine N4 atom appears coupled with the H5 proton at −64.8 ppm, and the hydrazinic/azomethinic N3 atom also coupled with the H5 proton through ^{3}J (6 Hz) at −206.0 ppm. The signal of the terminal thioamide function of the ligand, N1, is found at −269.1 ppm. In this case, the two protons of the amine groups are nonequivalent, and each is coupled with N1 through a strong coupling constant ^{1}J = 85−86 Hz. As can be seen in Table 3, the chemical shift of the terminal thioamide function appears in the −266 to −274.4 ppm range except for ligands HL^5 and H_2L^6 (labeled N7 and N10, respectively) which are found at −245.4 and −248.7 ppm due to the electronic effect of the cyclohexyl or aromatic group grafted on this thioamide. The hydrazinic nitrogen atom appears for all of the ligands in the range from −204.7 to −212.0 ppm. The nitrogen atom of the imine function falls in the range from −60.2 to −67.7 ppm, except for ligands HL^1 (−50.5 ppm), HL^2 (−53.1 ppm), and HL^7 (−46.1 ppm). The signals of N atoms belonging to the pyridine or quinoline moieties are in the same region in the range from −56.5 to −67.3 ppm.

Upon the formation of complexes (the major isomer), the latter are only slightly shifted up to +3.8 ppm, indicating that the pyridine/quinoline moieties of the ligands do not participate in the formation of complexes in almost all cases. In contrast, for the complex formed with ligand H_2L^6, the chemical shift of the N21 atom of the pyridine part undergoes a strong deshielding by 55.2 ppm which suggests coordination of Mo with the N21 atom, in agreement with the structure given in Figure 4.

Concerning the complexes formed with ligands HL^1, HL^2, and HL^7, the chemical shifts of the azomethinic N3 or N4 atoms are strongly affected with upfield ranging from 27.2 to 30.8 ppm, in accordance with the deprotonation and coordination of these atoms, while the imine nitrogen atoms are only slightly shifted by less than 3.8 ppm. These data agree well with the structures of complexes $[Mo_2O_2S_2(L^2)_2]$ and $[Mo_2O_2S_2(L^7)_2]$ (Figure 3) and suggest that the complex $[Mo_2O_2S_2(L^1)_2]$ possesses a similar molecular structure. The same features are evidenced for the complexes formed with phenolic derivatives $[Mo_2O_2S_2(HL^8)_2]$, $[Mo_2O_2S_2(H_2L^9)_2]$, $[Mo_2O_2S_2(H_2L^{10})_2]$, $[Mo_2O_2S_2(HL^{11})_2]$, and $[Mo_2O_2S_2(HL^{12})_2]$ with an upfield of the hydrazinic/azomethinic N group in the 28.4−30.9 ppm range while the imino N atom is slightly affected. Once again, this result agrees well with the molecular structures of complexes $[Mo_2O_2S_2(HL^8)_2]$ and $[Mo_2O_2S_2(HL^{12})_2]$ (Figure 5).

Interestingly, the ^{15}N NMR data of complexes $[Mo_2O_2S_2(L^3)_2]$, $[Mo_2O_2S_2(L^4)_2]$, and $[Mo_2O_2S_2(L^5)_2]$ evidence a strong chemical shift variation of the imine group from +35.0 to +39.1 ppm, while it is difficult to observe the signals of the hydrazinic atoms because there is no proton in the vicinity through at least three bonds in these molecules. This result demonstrates that for these three complexes the ligand is coordinated by thiolate and by N imino groups. In the three cases, the ligands were synthesized with 2-acetylpyridine, i.e., R2 = Me. The donor methyl group should enhance the basicity of the imine groups for coordination with Mo(V) centers which favors the coordination of this N atom. Nevertheless, considering the formation of up to 5 isomers for these three complexes, even if this mode of coordination is favored, the latter probably competes with that involving the hydrazinic N atoms.

This hypothesis is supported by the NMR experiments performed for complexes $[Mo_2O_2S_2(L^{13})_2]$ and $[Mo_2O_2S_2(L^{14})_2]$. Indeed, the ^{15}N NMR data recorded for both complexes suggest the coordination of the azomethinic N atoms while the imino group remains noncoordinated. It contrasts with the structure obtained for complex $[Mo_2O_2S_2(L^{13})_2]$ which displays coordination through imino N atoms (see Figure 6). This demonstrates the possibilities of the formation of complexes by the two modes of coordination of the ligands, and the consequence is that up to 8 isomers have been observed in solution (see Figures S99 and S112).

In summary, ^{15}N NMR data allow the identification of the coordination mode of ligands with the $[Mo_2O_2S_2]^{2+}$ clusters. All of the complexes except for one do not exhibit a coordination of the terminal thioamido group and of the aldehyde/ketone part of the ligand R1. The coordination of the thiolate groups appears obvious from the crystallographic

https://doi.org/10.1021/acsomega.2c00705
ACS Omega 2022, 7, 16547−16560

Table 3. Chemical Shift Values of Nitrogen Atoms in the Free Ligands and Complexes (Major Isomer Can Be Either *cis* or *trans* but the Nature of the Isomer Could Not Be Determined)

Scheme of ligand with labels of N atoms	^{15}N chemical shift of uncoordinated ligands (ppm)	^{15}N chemical shift in complexes (ppm)	variation upon coordination[a,b] (ppm)
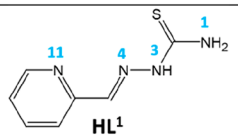 HL^1	N1: -267.2 N3: -205.7 N4: -50.5 N11: -62.4	N1: -261.3 N3: -178.5 N4: -33.1 N11: -60.5	N1: +5.9 **N3: +27.2** N4: +17.4 N11: +1.9
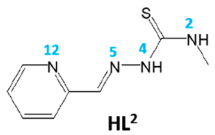 HL^2	N2: -272.0 N4: -206.6 N5: -53.1 N12: -63.0	N2: -269.6 N4: -178.6 N5: -36.1 N12: -60.8	N2: +2.4 **N4: +28.0** N5: +17.0 N12: +2.2
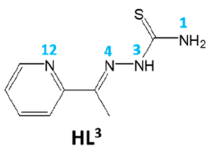 HL^3	N1: -266.4 N3: - N4: -62.5 N12: -66.2	N1: -262.9 N3: - N4: -27.5 N12: -	N1: +3.5 N3: - **N4: +35.0** N12: -
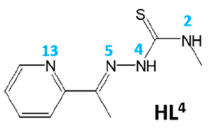 HL^4	N2: -271.1 N4: -212.0 N5: -64.9 N13: -67.3	N2: - N4: - N5: -27.6 N13: -	N2: - N4: - **N5: +37.3** N13: -
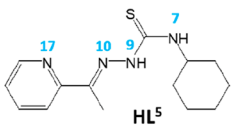 HL^5	N7: -245.4 N9: -212.0 N10: -65.6 N17: -66.2	N7: -243.5 N9: - N10: -26.5 N17: -	N7: +1.9 N9: - **N10: +39.1** N17: -
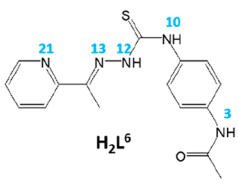 H_2L^6	N3: -244.2 N10: -248.7 N12: -209.2 N13: -65.3 N21: -67.0	N3: -244.2 N10: - N12: - N13: -48.6 N21: -122.2	N3: +0.0 N10: - N12: - N13: +16.7 **N21: +55.2**
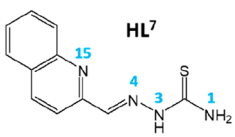 HL^7	N1: -267.2 N3: -205.0 N4: -46.1 N15: -67.3	N1: -260.6 N3: -177.1 N4: -28.8 N15: -63.5	N1: +6.6 **N3: +27.9** N4: +17.3 N15: +3.8
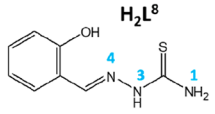 H_2L^8	N1: -269.1 N3: -206.0 N4: -64.8	N1: -263.1 N3: -177.6 N4: -47.8	N1: +6.0 **N3: +28.4** N4: +17.0
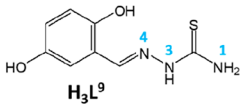 H_3L^9	N1: -270.1 N3: -206.2 N4: -65.4	N1: -261.0 N3: -175.3 N4: -47.4	N1: +9.1 **N3: +30.9** N4: +18.0
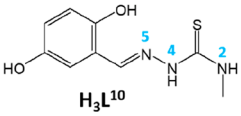 H_3L^{10}	N2: -274.4 N4: -207.5 N5: -67.3	N2: -271.0 N4: -178.0 N5: -48.7	N2: +3.4 **N4: +29.5** N5: +18.6

https://doi.org/10.1021/acsomega.2c00705
ACS Omega 2022, 7, 16547−16560

Table 3. continued

Scheme of ligand with labels of N atoms	^{15}N chemical shift of uncoordinated ligands (ppm)	^{15}N chemical shift in complexes (ppm)	variation upon coordination[a,b] (ppm)
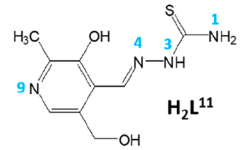 H_2L^{11}	N1: -266.8 N3: -204.7 N4: -60.2 N9: -56.5	N1: -261.0 N3: -175.3 N4: -47.4 N9: -53.1	N1: +5.8 **N3: +29.4** N4: +12.8 N9: +3.4
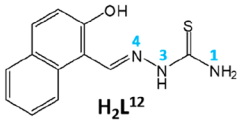 H_2L^{12}	N1: -269.3 N3: - 205.5 N4: - 67.7	N1: -263.5 N3: -174.7 N4: -56.3	N1: +5.8 **N3: +30.8** N4: +11.4
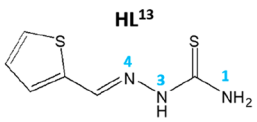 HL^{13}	N1: -271.0 N3: -207.6 N4: -66.3	N1: -264.3 N3: -178.6 N4: -47.2	N1: +6.7 **N3: +29.0** N4: +19.1
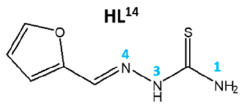 HL^{14}	N1: -269.9 N3: -206.5 N4: -64.9	N1: -261.9 N3: -176.9 N4: -45.5	N1: +8.0 **N3: +29.6** N4: +19.4

[a]Variation of chemical shifts observed for the major isomer. [b]The coordinated N atom is highlighted in bold red.

data and FT-IR spectra, and the coordination of the hydrazinic N atoms seems to be favored for the main part of our complexes. If so, only two isomers, *cis* and *trans*, are observed. On the contrary, when substituent R2 is a methyl group or when R1 is a furan or a thiophene group, a competition takes place between imino and thioamido N atoms to link the Mo^V centers. In this case, a complex mixture of 4−8 isomers in solution occurs. Such types of ligands should be avoided in further work to prevent the formation of complicated mixtures.

CONCLUSION

We have succeeded in isolating 14 new coordination complexes made by associating the cluster $[Mo_2O_2S_2]^{2+}$ with a collection of thiosemicarbazone ligands displaying various R1, R2, and R3 groups. MALDI-TOF experiments demonstrate that the powders obtained during the syntheses correspond to binuclear complexes of Mo(V) coordinated by two monoanionic thiosemicarbazone ligands. For the major part of complexes, single-crystal structural studies show unusual coordination modes of the thiosemicarbazone ligands through the thiolate groups and the azomethinic N atoms. In addition, the two ligands can take either a *cis* or a *trans* position with respect to the molybdenum block $[Mo_2O_2S_2]^{2+}$, in agreement with the NMR solution studies. In fact, most of the complexes exist in solution in two isomeric forms generally in unequal proportions. ^{15}N NMR studies allowed characterizations of the nitrogen atoms of ligands coordinated to the metallic centers in DMSO. This technique, rarely used, appears as an efficient tool to study such complexes in solution and provides important information about the coordination modes of thiosemicarbazone ligands for diamagnetic complexes. It also unambiguously highlights the nature of N atoms linked to the Mo centers for the major isomers. Through the 14 ligands used in this study, influences of the variation of the R1, R2, and R3 groups are also studied. It appears that, in all cases, R1 groups remain uncoordinated. Furthermore, when R1 is a furan or a thiophene derivative, the number of isomers in solution increases up to 8 isomers which have not been identified. The same effect is obtained when R2 = Me instead of H for ligands HL^3, HL^4, HL^5, and H_2L^6, which makes the solution studies more difficult. This could be due to an increase of the basicity of the imine group. Such ligands should thus be avoided in further work with $[Mo_2O_2S_2]^{2+}$ if we want to diminish the number of isomers. Our attention is now focused on biological properties of such coordination complexes and the chemical ways to favor the selective synthesis of one unique isomer for such types of complexes.

ASSOCIATED CONTENT

Supporting Information

The Supporting Information is available free of charge at https://pubs.acs.org/doi/10.1021/acsomega.2c00705.

Experimental Section; FT-IR spectra; MALDI-TOF spectra; crystallographic data with labeled molecular structures; NMR spectra; summary of NMR data; and possible isomers with two bidentate ligands involving the same coordinating atoms (PDF)

Crystallographic information files (CIF, CIF, CIF, CIF, CIF, CIF, CIF)

AUTHOR INFORMATION

Corresponding Authors

Aurelian Gulea − *State University of Moldova, Chişinău 2009, Republic of Moldova*; Email: guleaaurelian@gmail.com

Sébastien Floquet − *Institut Lavoisier de Versailles, CNRS UMR 8180, Univ. Versailles Saint Quentin en Yvelines, Université Paris-Saclay, 78035 Cedex Versailles, France*; orcid.org/0000-0003-2433-1771; Email: sebastien.floquet@uvsq.fr

Authors

Arcadie Fuior − *Institut Lavoisier de Versailles, CNRS UMR 8180, Univ. Versailles Saint Quentin en Yvelines, Université*

https://doi.org/10.1021/acsomega.2c00705
ACS Omega 2022, 7, 16547−16560

Paris-Saclay, 78035 Cedex Versailles, France; State University of Moldova, Chişinău 2009, Republic of Moldova

Diana Cebotari − *Institut Lavoisier de Versailles, CNRS UMR 8180, Univ. Versailles Saint Quentin en Yvelines, Université Paris-Saclay, 78035 Cedex Versailles, France; State University of Moldova, Chişinău 2009, Republic of Moldova*

Mohamed Haouas − *Institut Lavoisier de Versailles, CNRS UMR 8180, Univ. Versailles Saint Quentin en Yvelines, Université Paris-Saclay, 78035 Cedex Versailles, France;* orcid.org/0000-0002-2133-702X

Jérôme Marrot − *Institut Lavoisier de Versailles, CNRS UMR 8180, Univ. Versailles Saint Quentin en Yvelines, Université Paris-Saclay, 78035 Cedex Versailles, France*

Guillermo Minguez Espallargas − *Institute of Molecular Science, University of Valencia, 46980 Paterna, Spain;* orcid.org/0000-0001-7855-1003

Vincent Guérineau − *Institut de Chimie des Substances Naturelles, CNRS UPR2301, Université Paris-Saclay, 91198 Cedex Gif-sur-Yvette, France*

David Touboul − *Institut de Chimie des Substances Naturelles, CNRS UPR2301, Université Paris-Saclay, 91198 Cedex Gif-sur-Yvette, France;* orcid.org/0000-0003-2751-774X

Roman V. Rusnac − *State University of Moldova, Chişinău 2009, Republic of Moldova*

Complete contact information is available at: https://pubs.acs.org/10.1021/acsomega.2c00705

Notes

The authors declare no competing financial interest.

■ ACKNOWLEDGMENTS

University of Versailles, the "Institut Universitaire de France, IUF", and the CNRS are gratefully acknowledged for financial support. A.F. and D.C. gratefully acknowledge Campus France for Excellence Eiffel grant as well as State University of Moldova for funding their PhD theses. G.M.E. acknowledges the Blaise Pascal International Chair for financial support. This work is supported by the "ADI 2019" project funded by the IDEX Paris-Saclay, ANR-11-IDEX-0003-02, "Joint research projects AUF-MECR 2020-2021" funding program, and a public grant overseen by the French National Research Agency as part of the "Investissements d'Avenir" program (Labex Charm3at, ANR-11-LABX-0039-grant). The financial support from National Agency for Research and Development (ANCD) of the Republic of Moldova (Project 20.80009.5007.10) is also acknowledged.

■ REFERENCES

(1) Hille, R. Molybdenum and Tungsten in Biology. *Trends Biochem. Sci.* **2002**, *27* (7), 360−367.

(2) Maia, L. B.; Moura, I.; Moura, J. J. G. Molybdenum and Tungsten-Containing Enzymes: An Overview. In *Molybdenum and Tungsten Enzymes*; RSC, 2016; Chapter 1, pp 1−80.

(3) Gladyshev, V. N.; Zhang, Y. Abundance, Ubiquity and Evolution of Molybdoenzymes. In *Molybdenum and Tungsten Enzymes*; RSC, 2016; Chapter 2, pp 81−99.

(4) Nishino, T.; Okamoto, K.; Leimkühler, S. Enzymes of the Xanthine Oxidase Family. In *Molybdenum and Tungsten Enzymes*; RSC, 2016; Chapter 6, pp 192−239.

(5) Kappler, U.; Schwarz, G. The Sulfite Oxidase Family of Molybdenum Enzymes. In *Molybdenum and Tungsten Enzymes*; RSC, 2016; Chapter 7, pp 240−273.

(6) Seefeldt, L. C.; Dean, D. R.; Hoffman, B. M. Nitrogenase Mechanism: Electron and Proton Accumulation and N2 Reduction. In *Molybdenum and Tungsten Enzymes*; RSC, 2016; Chapter 8, pp 274−296.

(7) Yamase, T. Anti-Tumor, -Viral, and -Bacterial Activities of Polyoxometalates for Realizing an Inorganic Drug. *J. Mater. Chem.* **2005**, *15* (45), 4773−4782.

(8) Boulmier, A.; Feng, X.; Oms, O.; Mialane, P.; Riviere, E.; Shin, C. J.; Yao, J.; Kubo, T.; Furuta, T.; Oldfield, E.; Dolbecq, A. Anticancer Activity of Polyoxometalate-Bisphosphonate Complexes: Synthesis, Characterization, In Vitro and In Vivo Results. *Inorg. Chem.* **2017**, *56* (13), 7558−7565.

(9) Compain, J.-D.; Mialane, P.; Marrot, J.; Secheresse, F.; Zhu, W.; Oldfield, E.; Dolbecq, A. Tetra- to Dodecanuclear Oxomolybdate Complexes with Functionalized Bisphosphonate Ligands: Activity in Killing Tumor Cells. *Chem.- Eur. J.* **2010**, *16* (46), 13741−13748.

(10) Blazevic, A.; Rompel, A. The Anderson−Evans Polyoxometalate: From Inorganic Building Blocks via Hybrid Organic−Inorganic Structures to Tomorrows "Bio-POM. *Coord. Chem. Rev.* **2016**, *307*, 42−64.

(11) Ott, V. R.; Swieter, D. S.; Schultz, F. A. Di-.Mu.-Oxo, .Mu.-Oxo-.Mu.-Sulfido, and Di-.Mu.-Sulfido Complexes of Molybdenum(V) with EDTA, Cysteine, and Cysteine Ester Ligands. Preparation and Electrochemical and Spectral Properties. *Inorg. Chem.* **1977**, *16* (10), 2538−2545.

(12) Spivack, B.; Dori, Z. Structural aspects of Molybdenum(IV), Molybdenum(V) and molybdenum(VI) complexes. *Coord. Chem. Rev.* **1975**, *17* (2−3), 99−136.

(13) Gretarsdóttir, J. M.; Bobersky, S.; Metzler-Nolte, N.; Suman, S. G. Cytotoxicity Studies of Water Soluble Coordination Compounds with a $[Mo_2O_2S_2]^{2+}$ Core. *J. Inorg. Biochem.* **2016**, *160*, 166−171.

(14) Suman, S. G.; Gretarsdottir, J. M.; Penwell, P. E.; Gunnarsson, J. P.; Frostason, S.; Jonsdottir, S.; Damodaran, K. K.; Hirschon, A. Reaction Chemistry of the Syn-$[Mo_2O_2(\mu\text{-}S)_2(S_2)(DMF)_3]$ Complex with Cyanide and Catalytic Thiocyanate Formation. *Inorg. Chem.* **2020**, *59* (11), 7644−7656.

(15) Gretarsdottir, J. M.; Jonsdottir, S.; Lewis, W.; Hambley, T. W.; Suman, S. G. Water-Soluble Alpha-Amino Acid Complexes of Molybdenum as Potential Antidotes for Cyanide Poisoning: Synthesis and Catalytic Studies of Threonine, Methionine, Serine, and Leucine Complexes. *Inorg. Chem.* **2020**, *59* (24), 18190−18204.

(16) Suman, S. G.; Gretarsdottir, J. M.; Snaebjornsson, T.; Runarsdottir, G. R.; Penwell, P. E.; Brill, S.; Green, C. Cyanide Detoxification by Molybdenum Sulfur Complexes. *J. Biol. Inorg. Chem.* **2014**, *19*, S760.

(17) Fuior, A.; Hijazi, A.; Garbuz, O.; Bulimaga, V.; Zosim, L.; Cebotari, D.; Haouas, M.; Toderas, I.; Gulea, A.; Floquet, S. Screening of Biological Properties of $Mo^{V}_2O_2S_2$- and $Mo^{V}_2O_4$-Based Coordination Complexes: Investigation of Antibacterial, Antifungal, Antioxidative and Antitumoral Activities versus Growing of Spirulina Platensis Biomass. *J. Inorg. Biochem.* **2022**, *226*, 111627.

(18) Kang, S.; Shiota, Y.; Kariyazaki, A.; Kanegawa, S.; Yoshizawa, K.; Sato, O. Heterometallic Fe-III/K Coordination Polymer with a Wide Thermal Hysteretic Spin Transition at Room Temperature. *Chem.- Eur. J.* **2016**, *22* (2), 532−538.

(19) Floquet, S.; Boillot, M. L.; Riviere, E.; Varret, F.; Boukheddaden, K.; Morineau, D.; Negrier, P. Spin Transition with a Large Thermal Hysteresis near Room Temperature in a Water Solvate of an Iron(III) Thiosemicarbazone Complex. *New J. Chem.* **2003**, *27* (2), 341−348.

(20) Floquet, S.; Guillou, N.; Negrier, P.; Riviere, E.; Boillot, M.-L. The Crystallographic Phase Transition for a Ferric Thiosemicarbazone Spin Crossover Complex Studied by X-Ray Powder Diffraction. *New J. Chem.* **2006**, *30* (11), 1621−1627.

(21) Suvarapu, L. N.; Somala, A. R.; Koduru, J. R.; Baek, S. O.; Ammireddy, V. R. A Critical Review on Analytical and Biological Applications of Thio- and Phenylthiosemicarbazones. *Asian J. Chem.* **2012**, *24* (5), 1889−1898.

(22) Mckenzie-Nickson, S.; Bush, A. I.; Barnham, K. J. Bis-(Thiosemicarbazone) Metal Complexes as Therapeutics for Neurodegenerative Diseases. *Curr. Top. Med. Chem.* **2016**, *16* (27), 3058−3068.
(23) More, M. S.; Joshi, P. G.; Mishra, Y. K.; Khanna, P. K. Metal Complexes Driven from Schiff Bases and Semicarbazones for Biomedical and Allied Applications: A Review. *Mater. Today Chem.* **2019**, *14*, 100195.
(24) Merlot, A. M.; Kalinowski, D. S.; Richardson, D. R. Novel Chelators for Cancer Treatment: Where Are We Now? *Antioxid. Redox Signal.* **2013**, *18* (8), 973−1006.
(25) Yu, Y.; Kalinowski, D. S.; Kovacevic, Z.; Siafakas, A. R.; Jansson, P. J.; Stefani, C.; Lovejoy, D. B.; Sharpe, P. C.; Bernhardt, P. V.; Richardson, D. R. Thiosemicarbazones from the Old to New: Iron Chelators That Are More Than Just Ribonucleotide Reductase Inhibitors. *J. Med. Chem.* **2009**, *52* (17), 5271−5294.
(26) Matesanz, A.; Herrero, J. M.; Quiroga, A. G. Chemical and Biological Evaluation of Thiosemicarbazone-Bearing Heterocyclic Metal Complexes. *Curr. Top. Med. Chem.* **2021**, *21* (1), 59−72.
(27) Beraldo, H.; Gambino, D. The Wide Pharmacological Versatility of Semicarbazones, Thiosemicarbazones and Their Metal Complexes. *Mini-Rev. Med. Chem.* **2004**, *4* (1), 31−39.
(28) Kalinowski, D. S.; Quach, P.; Richardson, D. R. Thiosemicarbazones: The New Wave in Cancer Treatment. *Future Med. Chem.* **2009**, *1* (6), 1143−1151.
(29) Moharana, A. K.; Dash, R. N.; Subudhi, B. B. Thiosemicarbazides: Updates on Antivirals Strategy. *Mini-Rev. Med. Chem.* **2021**, *20* (20), 2135−2152.
(30) Shakya, B.; Yadav, P. N. Thiosemicarbazones as Potent Anticancer Agents and Their Modes of Action. *Mini-Rev. Med. Chem.* **2020**, *20* (8), 638−661.
(31) Carneiro Brum, J. de O.; Costa Franca, T. C.; Figueroa Villar, J. D. Synthesis and Biological Activity of Hydrazones and Derivatives: A Review. *Mini-Rev. Med. Chem.* **2020**, *20* (5), 342−368.
(32) Pessoa de Siqueira, L. R.; Teixeira de Moraes Gomes, P. A.; de Lima Ferreira, L. P.; Barreto de Melo Rego, M. J.; Lima Leite, A. C. Multi-Target Compounds Acting in Cancer Progression: Focus on Thiosemicarbazone, Thiazole and Thiazolidinone Analogues. *J. Med. Chem.* **2019**, *170*, 237−260.
(33) Haldys, K.; Latajka, R. Thiosemicarbazones with Tyrosinase Inhibitory Activity. *Medchemcomm* **2019**, *10* (3), 378−389.
(34) Scarim, C. B.; Jornada, D. H.; Machado, M. G. M.; Ferreira, C. M. R.; dos Santos, J. L.; Chung, M. C. Thiazole, Thio and Semicarbazone Derivatives against Tropical Infective Diseases: Chagas Disease, Human African Trypanosomiasis (HAT), Leishmaniasis, and Malaria. *Eur. J. Med. Chem.* **2019**, *162*, 378−395.
(35) Lima Leite, A. C.; Pontes Espindola, J. W.; de Oliveira Cardoso, M. V.; de Oliveira Filho, G. B. Privileged Structures in the Design of Potential Drug Candidates for Neglected Diseases. *Curr. Med. Chem.* **2019**, *26* (23), 4323−4354.
(36) Summers, K. L. A Structural Chemistry Perspective on the Antimalarial Properties of Thiosemicarbazone Metal Complexes. *Mini-Rev. Med. Chem.* **2019**, *19* (7), 569−590.
(37) Heffeter, P.; Pape, V. F. S.; Enyedy, E. A.; Keppler, B. K.; Szakacs, G.; Kowol, C. R. Anticancer Thiosemicarbazones: Chemical Properties, Interaction with Iron Metabolism, and Resistance Development. *Antioxid. Redox Signal.* **2019**, *30* (8), 1062−1082.
(38) Liang, J.-X.; Zhong, H.-J.; Yang, G.; Vellaisamy, K.; Ma, D.-L.; Leung, C.-H. Recent Development of Transition Metal Complexes with in Vivo Antitumor Activity. *J. Inorg. Biochem.* **2017**, *177*, 276−286.
(39) Pahontu, E.; Julea, F.; Rosu, T.; Purcarea, V.; Chumakov, Y.; Petrenco, P.; Gulea, A. Antibacterial, Antifungal and in Vitro Antileukaemia Activity of Metal Complexes with Thiosemicarbazones. *J. Cell. Mol. Med.* **2015**, *19* (4), 865−878.
(40) Rosu, T.; Negoiu, M.; Pasculescu, S.; Pahontu, E.; Poirier, D.; Gulea, A. Metal-Based Biologically Active Agents: Synthesis, Characterization, Antibacterial and Antileukemia Activity Evaluation of Cu(II), V(IV) and Ni(II) Complexes with Antipyrine-Derived Compounds. *Eur. J. Med. Chem.* **2010**, *45* (2), 774−781.
(41) Pahonţu, E.; Julea, F.; Chumakov, Y.; Petrenco, P.; Roşu, T.; Gulea, A. Synthesis, Characterization, Crystal Structure and Antiproliferative Activity Studies of Cu(II), Ni(II) and Co(II) Complexes with 4-Benzoyl-5-Pyrazolones Derived Compounds. *J. Organomet. Chem.* **2017**, *836*−*837*, 44−55.
(42) Rosu, T.; Pahontu, E.; Ilies, D.-C.; Georgescu, R.; Mocanu, M.; Leabu, M.; Shova, S.; Gulea, A. Synthesis and Characterization of Some New Complexes of Cu(II), Ni(II) and V(IV) with Schiff Base Derived from Indole-3-Carboxaldehyde. Biological Activity on Prokaryotes and Eukaryotes. *Eur. J. Med. Chem.* **2012**, *53*, 380−389.
(43) Pahontu, E.; Fala, V.; Gulea, A.; Poirier, D.; Tapcov, V.; Rosu, T. Synthesis and Characterization of Some New Cu(II), Ni(II) and Zn(II) Complexes with Salicylidene Thiosemicarbazones: Antibacterial, Antifungal and in Vitro Antileukemia Activity. *Molecules* **2013**, *18* (8), 8812−8836.
(44) Gulea, A.; Poirier, D.; Roy, J.; Stavila, V.; Bulimestru, I.; Tapcov, V.; Birca, M.; Popovschi, L. In Vitro Antileukemia, Antibacterial and Antifungal Activities of Some 3d Metal Complexes: Chemical Synthesis and Structure - Activity Relationships. *J. Enzyme Inhib. Med. Chem.* **2008**, *23* (6), 806−818.
(45) Eglence, S.; Sahin, M.; Ozyurek, M.; Apak, R.; Ulkuseven, B. Dioxomolybdenum(VI) Complexes of S-Methyl-5-Bromosalicylidene-N-Alkyl Substituted Thiosemicarbazones: Synthesis, Catalase Inhibition and Antioxidant Activities. *Inorg. Chim. Acta* **2018**, *469*, 495−502.
(46) Eglence-Bakir, S.; Sacan, O.; Sahin, M.; Yanardag, R.; Ulkuseven, B. Dioxomolybdenum(VI) Complexes with 3-Methoxy Salicylidene-N-Alkyl Substituted Thiosemicarbazones. Synthesis, Characterization, Enzyme Inhibition and Antioxidant Activity. *J. Mol. Struct.* **2019**, *1194*, 35−41.
(47) Eglence-Bakir, S.; Sahin, M.; Zahoor, M.; Dilmen-Portakal, E.; Ulkuseven, B. Synthesis and Biological Potentials of Dioxomolybdenum(VI) Complexes with ONS and ONN Chelating Thiosemicarbazones: DNA-Binding. *Antioxidant and Enzyme Inhibition Studies. Polyhedron* **2020**, *190*, 114754.
(48) Garg, R.; Kumari, A.; Joshi, S. C.; Fahmi, N. Manganese(II) and Dioxomolybdenum(VI) Complexes with Monobasic Bidentate Schiff Bases: Synthesis, Characterization and Biological Investigation. *Bull. Korean Chem. Soc.* **2013**, *34* (8), 2381−2386.
(49) Vrdoljak, V.; Đilović, I.; Rubčić, M.; Kraljević Pavelić, S.; Kralj, M.; Matković-Čalogović, D.; Piantanida, I.; Novak, P.; Rožman, A.; Cindrić, M. Synthesis and Characterisation of Thiosemicarbazonato Molybdenum(VI) Complexes and Their in Vitro Antitumor Activity. *Eur. J. Med. Chem.* **2010**, *45* (1), 38−48.
(50) Elsayed, S. A.; Noufal, A. M.; El-Hendawy, A. M. Synthesis, Structural Characterization and Antioxidant Activity of Some Vanadium(IV), Mo(VI)/(IV) and Ru(II) Complexes of Pyridoxal Schiff Base Derivatives. *J. Mol. Struct.* **2017**, *1144*, 120−128.
(51) Celen, S.; Eglence-Bakir, S.; Sahin, M.; Deniz, I.; Celik, H.; Kizilcikli, I. Synthesis and Characterization of New Thiosemicarbazonato Molybdenum(VI) Complexes and Their in Vitro Antimicrobial Activities. *J. Coord. Chem.* **2019**, *72* (10), 1747−1758.
(52) Pisk, J.; Prugovecki, B.; Matkovic-Calogovic, D.; Poli, R.; Agustin, D.; Vrdoljak, V. Charged Dioxomolybdenum(VI) Complexes with Pyridoxal Thiosemicarbazone Ligands as Molybdenum(V) Precursors in Oxygen Atom Transfer Process and Epoxidation (Pre)Catalysts. *Polyhedron* **2012**, *33* (1), 441−449.
(53) Vrdoljak, V.; Milic, D.; Cindric, M.; Matkovic-Calogovic, D.; Pisk, J.; Markovic, M.; Novak, P. Synthesis, Structure and Characterization of Dinuclear Pentacoordinate Molybdenum(V) Complexes with Thiosemicarbazone Ligands. *Z. Anorg. Allg. Chem.* **2009**, *635* (8), 1242−1248.
(54) Vrdoljak, V.; Pisk, J.; Prugovecki, B.; Matkovic-Calogovic, D. Novel Dioxomolybdenum(VI) and Oxomolybdenum(V) Complexes with Pyridoxal Thiosemicarbazone Ligands: Synthesis and Structural Characterisation. *Inorg. Chim. Acta* **2009**, *362* (11), 4059−4064.

https://doi.org/10.1021/acsomega.2c00705
ACS Omega 2022, 7, 16547−16560

(55) Vrdoljak, V.; Milic, D.; Cindric, M.; Matkovic-Calogovic, D.; Cincic, D. Synthesis of Novel Molybdenum(V) Complexes: Structural Characterization of Two Thiosemicarbazonato Complexes $[MoOCl_2\{C_6H_4(O)CH:NNHC:SNHC_6H_5\}]$ and $[MoOCl_2\{C_{10}H_6(O)CH:NNHC:SNHC_6H_5\}].CH_3CN$, and Two Oxohalomolybdates $NH_4[MoOCl_4(CH_3CN)]$ and $[C_5H_5NH]_2[MoOCl_5]$-CH_2Cl_2. *Polyhedron* **2007**, *26* (13), 3363−3372.
(56) Cadot, E.; Sokolov, M. N.; Fedin, V. P.; Simonnet-Jegat, C.; Floquet, S.; Secheresse, F. A Building Block Strategy to Access Sulfur-Functionalized Polyoxometalate Based Systems Using $\{Mo_2S_2O_2\}$ and $\{Mo_3S_4\}$ as Constitutional Units, Linkers or Templates. *Chem. Soc. Rev.* **2012**, *41* (22), 7335−7353.
(57) Lemonnier, J.-F.; Duval, S.; Floquet, S.; Cadot, E. A Decade of Oxothiomolybdenum Wheels: Synthesis, Behavior in Solution, and Electrocatalytic Properties. *Isr. J. Chem.* **2011**, *51* (2), 290−302.
(58) Floquet, S.; Munoz, M. C.; Guillot, R.; Riviere, E.; Blain, G.; Real, J.-A.; Boillot, M.-L. A Wide Family of Pyridoxal Thiosemicarbazone Ferric Complexes: Syntheses, Structures and Magnetic Properties. *Inorg. Chim. Acta* **2009**, *362* (1), 56−64.
(59) Cindric, M.; Vrdoljak, V. N.; Strukan, N.; Kamenar, B. Synthesis and Characterization of Some Mono- and Dinuclear Molybdenum(VI) Thiosemicarbazonato Complexes. *Polyhedron* **2005**, *24* (2), 369−376.
(60) Cadot, E.; Salignac, B.; Marrot, J.; Dolbecq, A.; Secheresse, F. $[Mo_{10}S_{10}O_{10}(OH)_{10}(H_2O)_5]$: A Novel Decameric Molecular Ring Showing Supramolecular Properties. *Chem. Commun.* **2000**, *4*, 261−262.
(61) Vojinović-Ješić, L.; Leovac, V.; Radanović, M.; Češljević, V.; Jovanović, L.; Rodić, M.; Divjaković, V. Transition Metal Complexes with Thiosemicarbazide-Based Ligands, Part 58. Synthesis, Spectral and Structural Characterization of Dioxovanadium (V) Complexes with···. *J. Serbian Chem. Soc.* **2011**, *76*, 865−877.
(62) Massiot, D.; Fayon, F.; Capron, M.; King, I.; Le Calvé, S.; Alonso, B.; Durand, J.-O.; Bujoli, B.; Gan, Z.; Hoatson, G. Modelling One- and Two-Dimensional Solid-State NMR Spectra: Modelling 1D and 2D Solid-State NMR Spectra. *Magn. Reson. Chem.* **2002**, *40* (1), 70−76.
(63) Venkatachalam, T. K.; Pierens, G. K.; Reutens, D. C. Synthesis, NMR Structural Characterization and Molecular Modeling of Substituted Thiosemicarbazones and Semicarbazones Using DFT Calculations to Prove the Syn/Anti Isomer Formation. *Magn. Reson. Chem.* **2014**, *52* (3), 98−105.
(64) Floquet, S.; Brun, S.; Lemonnier, J.-F.; Henry, M.; Delsuc, M.-A.; Prigent, Y.; Cadot, E.; Taulelle, F. Molecular Weights of Cyclic and Hollow Clusters Measured by DOSY NMR Spectroscopy. *J. Am. Chem. Soc.* **2009**, *131* (47), 17254−17259.
(65) Duval, S.; Floquet, S.; Simonnet-Jegat, C.; Marrot, J.; Biboum, R. N.; Keita, B.; Nadjo, L.; Haouas, M.; Taulelle, F.; Cadot, E. Capture of the $[Mo_3S_4]^{4+}$ Cluster within a {Mo-18} Macrocycle Yielding a Supramolecular Assembly Stabilized by a Dynamic H-Bond Network. *J. Am. Chem. Soc.* **2010**, *132* (6), 2069−2077.
(66) Köck, M.; Junker, J.; Lindel, T. Impact of the $^{1}H,^{15}N$-HMBC Experiment on the Constitutional Analysis of Alkaloids. *Org. Lett.* **1999**, *1* (13), 2041−2044.
(67) Marek, R.; Lycka, A. ^{15}N NMR Spectroscopy in Structural Analysis. *Curr. Org. Chem.* **2002**, *6* (1), 35−66.

https://doi.org/10.1021/acsomega.2c00705
ACS Omega 2022, 7, 16547−16560